DYNAMIC TENSILE STRENGTH OF PMMA/AL PLATE BUTT ADHESIVE JOINTS

H. WADA[*1], S. KUBO[*1] K. MURASE[*2] and T. C. KENNEDY[*3]

*1 Daido Institute of Technology, 10-3 Takiharu-cho, Minami-ku, Nagoya, 457-8530 Japan
*2 Meijo University, Tenpaku, Nagoya, 468-8502 Japan
*3 Oregon State University, Corvallis, OR 97331-5001 USA

ABSTRACT

The impact strength was evaluated for a butt adhesive joint of Al alloy plate and PMMA plate. The materials were bonded together by cold-setting epoxy, commercial base adhesive. An impact tension test was carried out using a drop-weight testing machine. The fracture initiation time in the adhesive interface was determined from the measured strain gage signal. The impact tensile strengths of the adhesive joint were evaluated by the stress singularity field parameter and the average fracture stress. Fracture toughness in the dynamic stress field was determined from the stress distribution in the vicinity of the edge of the adhesive interface calculated by the finite element method at the fracture initiation time. The static fracture toughness was also determined by a similar method using the same type of specimen used in the dynamic test. It was found that the dynamic strengths exhibited considerably larger values than the static strengths.

KEYWORDS: Dynamic tensile strength, Butt adhesive joint, Adhesively bonded dissimilar butt joints, Loading rate, Stress singularity, Strain gage, Finite element method

INTRODUCTION

Recently, adhesive technology has been introduced into a wide variety of fields for the purpose of lightening and cost reduction of machine structures. However, the establishment of a fracture criterion for the adhesive interface which is useful for design is a difficult task, because of the wide variability of strength. So far, studies[(1)~(5)] on stress analysis and strength evaluation of the adhesive interface have been carried out mainly for the static problem with the development of the numerical analysis technology. In particular, the followings are reported for the strength evaluation: methods based on maximum stress, methods based the stress singularity field parameter at a joint of dissimilar materials, and methods based on fracture mechanics including a crack, etc. Generally it is known that a singularity in the stress appears in the vicinity of the edge in the adhesive interface between dissimilar materials. Therefore, a strength evaluation method based on the stress singularity field parameter[(3)] for the adhesive joint between dissimilar materials has been proposed for the static problem. The establishment of an impact strength evaluation method for an adhesive joint is needed for the case of severe loading of the structure. In this study, the dynamic tensile strengths are investigated for the dissimilar butt adhesive joints with the fracture toughness and the average fracture stress.

EXPERIMENTAL METHOD

MATERIALS AND SPECIMEN

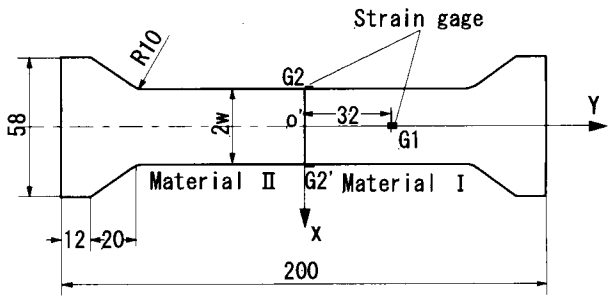

2w=30 h=6 (Dimensions in mm)

Fig.1 Specimen configuration and dimensions.

Table 1 Physical properties of materials.

		Young's modulus E (GPa)	Density ρ (kg/m^3)	Poisson's ratio ν
PMMA	Dynamic	4.87	1.18×10^3	0.388
	Static	3.50		
Al alloy	Dynamic	71.8	2.70×10^3	0.331
	Static			

The specimen configuration used in this experiment is shown in Fig.1. The specimen thickness was h=6mm. PMMA was used for Material I, and Al alloy (A6061P-T6) was used for Material II. The physical properties of both adherents are shown in Table1. A strain gage was bonded in the center (G1) of the Material I side (PMMA) shown in Fig.1 in order to measure the time-history of the stress in the specimen. Strain gages were also bonded in the vicinity of the edge of the adhesive interface (G2, G2') in order to measure the fracture initiation time. In this way, the time-history of strain measured by the strain gage (G1) was used as an external force for dynamic stress analysis by the finite element method. The two materials were bonded together using a special jig developed in this study in order to avoid slippage of the butt and non-uniformity of the thickness of the adhesive layer. The materials were bonded together by a cold-setting epoxy type adhesive (Epoxy resin 100%, Polyamide resin 100%). The specimen was used in the experiment after allowing the adhesive to set for 24 hours. Although the physical properties of the adhesive were not given by the manufacturer, the literature (3) gives physical properties for the same type of adhesive. Therefore, it was assumed that the physical properties of the adhesive used in this study were approximately equal to physical properties of the PMMA material of the adherent. Planes to adhere the two materials were polished in random directions by sandpaper. The surface roughness of the plane was measured with a surface roughness meter. As a result, the center line average roughness was R_a=0.12 μm for the PMMA material, R_a=0.14 μm for the Al alloy. By expanding with a projector by a factor of 20, the thickness of the adhesive layer of the joint was measured as about 50 μm.

IMPACT LOADING EQUIPMENT

The tension jig for impact tensile loading of the specimen is shown in Fig.2. It is constructed using 4 steel disks (ϕ160×30) and 8 steel pins (ϕ20×260), as shown in the figure. Steel disks 1 and 3, and 2 and 4 of the jig are respectively moved together by the pins. The specimen is installed in the center hole of steel disks 2 and 3. Disks 1 and 3 move downward when the falling weight collides with steel disk 1, and the specimen installed between disks 2 and 4 is dynamically pulled. The falling weight in the pipe is pulled up using a wire, and then, it is made to fall freely from some height in the tension jig. The largest height of the falling weight in this equipment is 1.6m. All experiments were carried out with the height of the weight at 0.8m. As the result, the velocity of the falling weight at

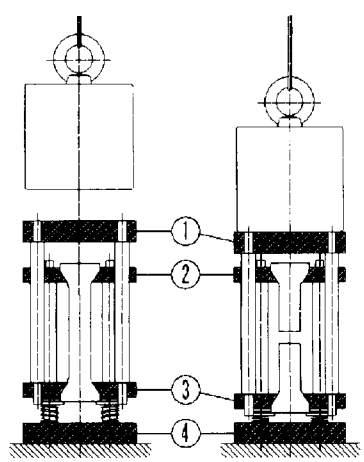

Fig.2 Impact tension jig.

the time of collision with the tension jig was about 4m/s. Also, a rubber plate of 5mm thickness was laid on disk 1 of the tension jig in order to reduce vibrations of high order caused by the collision of the falling weight.

DYNAMIC STRAIN MEASUREMENT

The dynamic strain measuring device system is shown in Fig.3. The output signal from the resistance strain gage which is bonded to specimen is converted into a voltage output by the bridge box, as shown in Fig.1. The voltage output is amplified by an amplifier (Signal conditioner CDV/CDA-230C, KYOWA). The time-history of the voltage output is recorded in the wave recorder (Transient converter TCL-005-DG, 6ch, 4096word/cha, 10bit smallest sampling time 50ns/W). It is also converted into strain after it is transferred to a personal computer. Incidentally, the strain measurement was carried out at a 200kHz digital sampling rate without using a filter in this experiment.

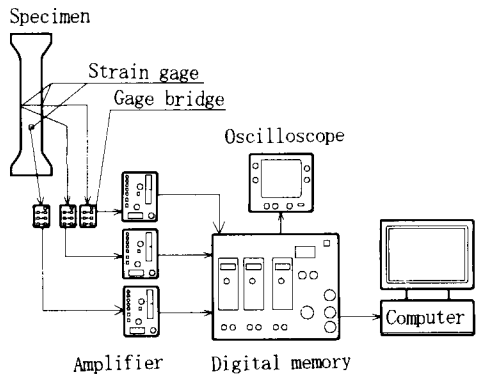

Fig.3 Recording system of dynamic strains.

DYNAMIC STRESS ANALYSIS BY FEM

Static and dynamic stresses in the adhesive joint between the dissimilar materials used in this experiment were analyzed using the general-purpose program ANSYS5.6. A second-order quadrilateral element with 8 nodes was used in the calculation, and the stress analysis was carried out with the assumption of plane stress conditions. Considering the symmetry of the specimen, only half of it was modeled. Fig.4(a) shows the boundary conditions on the specimen used to simulate the impact tension test in the FEM analysis. The time-history of the strain measured by the strain gauge G1 was used as a dynamic input load to the specimen. In this way, it was confirmed that the dynamic stress analyzed by the FEM agreed well with the measurement result. Therefore, numerical analysis by this method is appropriate. Fig.4(b) shows the element mesh of the specimen. The number of elements is 1571, and the number of the node is 4936. There is a singularity in stress at the edge of the adhesive joint interface, and it is necessary to divide this region into very small elements, since a large stress gradient exists. Fig.4(c) shows the details of the element mesh in the vicinity of the edge of the adhesive interface. The smallest element size is 19μm.

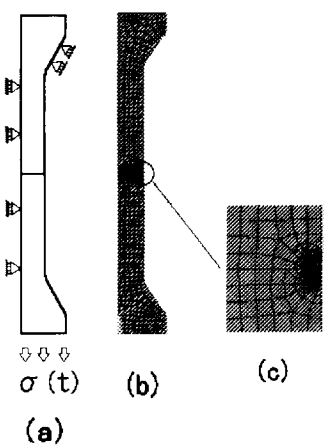

Fig.4 Boundary and meshing conditions.

STRESS SINGULARITY FIELD PARAMETER

The static stress distribution in the vicinity of the edge of an interface between dissimilar materials has been determined by Bogy[6]. Namely, the stress distribution is given in equation (1),

$$\sigma(x) = K / x^{\lambda} \tag{1}$$

where σ(x) is the stress component, K is the stress singularity field strength, and λ[7] is the exponent in the singular term which is determined by a combination of the properties of the dissimilar materials, and x is the distance along the interface from the singular point. The convenient technique shown next was used in order to determine the intensity K of the singular stress field. Namely, it is possible to obtain the theoretical resultant force F_y in a small region (a~c, a<b<c) in the vicinity of the singular point from Eq. (1) according to the following equation.

$$F_y = \int_a^c \frac{K}{x^{\lambda}} h \cdot dx \tag{2}$$

On the other hand, the stress in the 3 nodes of the 2 elements in the vicinity of the interface edge gives the resultant force F_{yf} from the finite element analysis by equation (3).

$$F_{yf} = \{\sigma_a + \sigma_b)(a - b) + (\sigma_b + \sigma_c)(b - c)\}h/2 \tag{3}$$

Equations (2) and (3) become equal, if the stress in the vicinity of the edge of the adhesion boundary is obtained accurately by the finite element method. Namely,

$$F_{yf} = F_y \tag{4}$$

Therefore, Eq.(5) is obtained from Eq.(4), and it is possible to conveniently obtain the intensity of the singular stress field from this equation

$$K = \{\sigma_a + \sigma_b)(a - b) + (\sigma_b + \sigma_c)(b - c)\}(1 - \lambda)/\{2(c^{1-\lambda} - a^{1-\lambda})\} \tag{5}$$

The value calculated by Eq.(5) was compared with the results from the extrapolation method in order to examine the accuracy of calculating the intensity K of the singular stress field. Good agreement was found, and it was confirmed that the convenient calculation formula given by Eq.(5) was effective.

RESULTS AND DISCUSSIONS

DYNAMIC STRESS

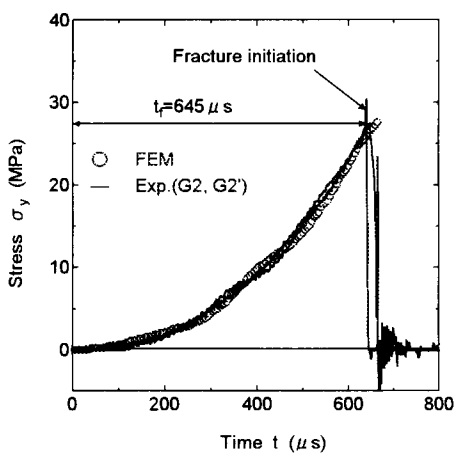

Fig.5 Dynamic stress response in adhesive joint

Figure 5 shows the results of simulating stress wave propagation in the specimen by the FEM. The measured results for the stress are also displayed in the figure for comparison with the calculation results. In the figure, the time-histories of stress measured by strain gages G2 and G2' are shown with the continuous line, and the calculation results by the FEM are shown with the mark o. Strain gages G2 and G2' were bonded on the edge of the PMMA material about 1.0mm from the adhesive interface. The two results are in good agreement until the stress rapidly decreases, as shown in the figure. Therefore, the dynamic stress which propagates in the specimen can be simulated by FEM accurately. In addition, the stress distribution at the adhesive interface at the fracture initiation time can be determined by the FEM analysis, as the strain gage signal yields the fracture initiation time value. Finally, the singular stress field parameter is obtained

from the stress distribution at the adhesive interface by FEM analysis.

IMPACT TENSILE STRENGTH

Fig.6 shows a Weibull plot[8] of the critical intensity of the stress field determined from stress component σ_y. A cumulative fracture probability F(%) of each data point was determined using the median rank method. There is considerable difference in the longitudinal modulus of elasticity of the PMMA material for the static value as compared to the dynamic one, as was shown in Table 1. Therefore, the value of the exponent λ of the singularity of the PMMA/Al adhesive joint specimen used in this experiment is different in the dynamic and static cases. Namely, it becomes λ=0.229 in the dynamic stress field, and it becomes λ=0.231 in the static stress field. The increase of λ becomes a factor which lowers the fracture strength. There is a difference evidently in the strength of the joint in the static case as compared to the dynamic one, as shown in the figure. The dynamic tensile strength of the PMMA/Al adhesion plate joint is considerably larger than the static strength. Namely, K_{yd} values are about 2.9 times those of K_{yc}. The interaction of the delay of the lateral deformation and the restraint of the deformation of PMMA material in the adhesive interface by the Al alloy, etc. appears to be the cause, since the velocity of the longitudinal wave is different from that of the transverse wave. Fig.7 shows critical intensities K_{xyc} and K_{xyd} of the singular stress field obtained from shearing stress τ_{xy}. Although K_{xy} is considerably smaller than K_y, the tendencies of the results in Fig.7 are similar to those of Fig.6 when comparing static and dynamic values. The dynamic tensile strength of the PMMA/Al adhesive joint is about 2.6 times that of the static strength.

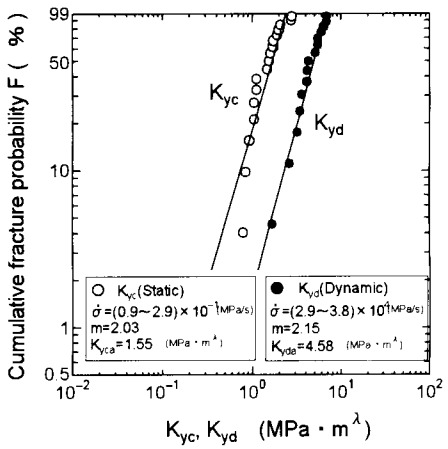

Fig.6 Weibull distributions of K_{yc}, K_{yd}

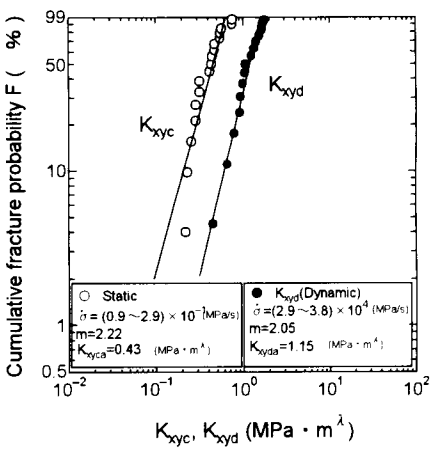

Fig.7 Weibull distributions of K_{xyc}, K_{xyd}

Fig.8 shows static fracture strengths of the joints for several combinations of materials on the average fracture stress on adhesive interface. The joint of Al/Al is highest strength due to the stiffening effect for adhesive layer by Al alloy. However, the strength of the PMMA/Al joint is lower than that of the PMMA/PMMA joint since it shows the stress singularity field. On the other hand, the dynamic strength of the PMMA/Al joint is higher than that of the PMMA/PMMA

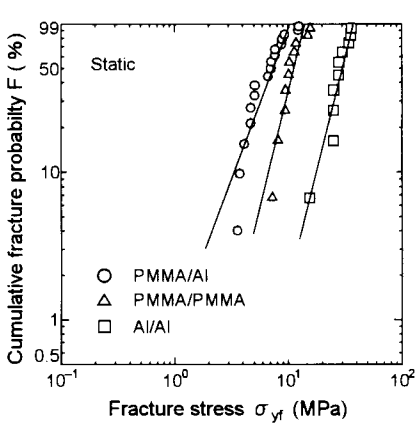

Fig.8 Weibull distributions of σ_{yc}

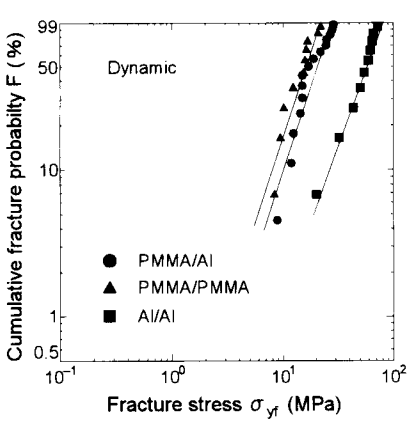

Fig.9 Weibull distributions of σ_{yd}

other hand, the dynamic strength of the PMMA/Al joint is higher than that of the PMMA/PMMA

joint slightly, as shown in Fig.9. Table 2 shows each numerical result relating both figures.

Table 2 Results of statistical analysis.

		Stress rate (MPa/s)	m	Average fracture stress σ_{yco}, σ_{yde} (MPa)
PMMA/Al	Static ○	$(0.9\sim2.9)\times10^{-1}$	2.04	6.97
	Dynamic ●	$(2.9\sim3.8)\times10^{4}$	2.27	18.98
PMMA/PMMA	Static △	$(0.9\sim1.2)\times10^{-1}$	3.09	10.78
	Dynamic ▲	$(1.8\sim4.0)\times10^{4}$	2.37	14.70
Al/Al	Static □	$(1.5\sim1.8)\times10^{-1}$	3.21	28.26
	Dynamic ■	$(1.8\sim8.0)\times10^{5}$	2.30	53.20

CONCLUSION

From the above results, the impact strength of a PMMA/Al plate butt adhesive joint was evaluated from a stress analysis by FEM and by measurement of fracture initiation time by strain gages, with the stress singularity field parameter and the average fracture stress. In addition, stress rate dependence of the strength of an adhesive joint between dissimilar materials was investigated in detail. Consequently, if some main clarified matters are considered, the following conclusions are derived.

(1) From the signal of a strain gage bonded to the specimen in the vicinity of the adhesive interface, it was possible to accurately determine the fracture initiation time in the specimen adhesive interface edge.

(2) In both the static and dynamic tests, fracture was observed to occur in the PMMA/epoxy adhesion interface.

(3) Using the fracture initiation time determined from the strain gage signal and the simulation results from the dynamic stress analysis by FEM, an effective technique for determining the singular stress field parameter at the fracture initiation time was developed.

(4) The dynamic tensile strengths of the PMMA/Al butt adhesion plate joint evaluated were about 2.9 times the static values for K_{yd}, and about 2.7 times the static values for σ_{yd}.

REFERENCES

(1) Sawa, T., K. Nakano, H. Toratani and M. Horiuchi, (1995). Two-Dimensional Stress Analysis of Single-Lap Adhesive Joints Subjected to Tensile Shear Loads. *Trans. of the JSME(A)*, **61**, 1994-2002.

(2) Tong, L., (1998). Strength of Adhesively Bonded Single-Lap and Lap-Shear Joints. *Int. J. Solids Structures*, **35**, 2601-2616.

(3) Hattori T., S. Sakata, T. Hatsuda and G. Murakami, (1988). A Stress Singularity Parameters Approach for Evaluating Adhesive Strength. *Trans. of the JSME(A)*, **54**, 597-602.

(4) Sato C., H. Iwata and K. Ikegami, (1997). Dynamic Strength of Adhesive Layer under Combined Impact Loading using Clamped Hopkinson Bar Method. *Trans. of the JSME(A)*, **63**, 341-346.

(5) Yokoyama T. and H. Shimizu, (1997). Determination of Impact Shear Strength of Adhesive Bonds with the Split Hopkinson Bar. *Trans. of the JSME(A)*, **63**, 2604-2609.

(6) Bogy D. B., (1971). Two Edge-Bonded Elastic Wedges of Different Materials and Wedge Angles Under Surface Tractions. *J. Appl. Mech.* **38**, 377-386.

(7) Dunders J., (1967). Effect of Elastic Constants on Stress in a Composite under Plane Deformations. *J. Composite Materials*, **1**, 310.

(8) Daimaruya M., H. Kobayashi, M. Chiba and H. Maeda, (1997). Measurement of Impact Tensile Strength of Concretes. *Trans. of the JSME(A)*, **63**, 2592-2597.